CT features of HER2-mutant lung adenocarcinomas

Peter Sawan[a,*], Andrew J. Plodkowski[a], Angela E. Li[a], Bob T. Li[b], Alexander Drilon[b,c], Marinela Capanu[d], Michelle S. Ginsberg[a]

[a]Department of Radiology, Memorial Sloan Kettering Cancer Center, 1275 York Avenue, New York, NY 10065, USA

[b]Thoracic Oncology Service, Division of Solid Tumor Oncology, Department of Medicine, Memorial Sloan Kettering Cancer Center, 1275 York Avenue, New York, NY 10065, USA

[c]Weill Cornell Medical College, 1300 York Avenue, New York, NY 10065, USA

[d]Department of Epidemiology and Biostatistics, Memorial Sloan Kettering Cancer Center, 1275 York Avenue, New York, NY 10065, USA

Abstract

Objectives: To describe the radiological phenotype of *HER2*-mutant lung cancers on CT at presentation.

Methods: Eligible patients with lung adenocarcinomas with *HER2* mutations were stage-matched with two control groups (*EGFR*- and *KRAS*-mutant groups). Evaluated CT features of the primary tumor included size, location, consistency, contour, presence of pleural tags and pleural retractions. Presence of pleural effusions, lung metastases, adenopathy, chest wall invasion, and were also recorded. Wilcoxon rank-sum and Fisher's exact tests were used to compare continuous and categorical features, respectively.

Results: One hundred and fifty-four patients were identified: 50 (33%) harbored *HER2* mutations, 56 (36%) harbored *KRAS* mutations, and 48 (31%) harbored *EGFR* mutations. Compared with *KRAS, HER2* tumors presented as smaller lesions (2.3 cm versus 2.9 cm, $p = 0.005$ for length; 1.6 cm versus 2.1 cm, $p = 0.002$ for width) with the presence of pleural tags (74% vs. 52%, $p = 0.03$), pleural retractions (58% vs. 39%, $p = 0.006$), ipsilateral hilar (36% vs. 16%, $p = 0.03$) and scalene/supraclavicular N3 adenopathy (24% vs. 7%, $p = 0.03$). Compared with *EGFR,* pleural retractions were more prevalent among the *HER2* tumors (58% vs. 37%, $p = 0.05$).

Conclusions: Lung adenocarcinomas with *HER2* gene mutation exhibit an aggressive behavior manifesting by higher incidence of local invasion, compared to *KRAS* and *EGFR* mutant controls, and a nodal metastatic spread compared to *KRAS*-mutant control. This is the first radiogenomics study of *HER2* mutations in lung cancer.

*Corresponding author. sawanp@mskcc.org (P. Sawan).

Keywords

Lung adenocarcinoma; Radiogenomics; Multidetector computed tomography; *HER2* ; *EGFR* ; *KRAS*

1. Introduction

Lung cancer remains the leading cause of cancer death worldwide, accounting for 1.69 million deaths in 2015 and approximately 19% of the total cancer death toll according to the World Health Organization [1]. In the United States, the American Cancer Society estimated that 222,500 new cases of lung cancer will be diagnosed in 2017, with an estimated mortality of 70% (155,870 deaths) among both sexes [2]. Of the two main types of lung cancer, non-small cell lung cancer comprises 80 to 85% of lung cancers and histologically, 40% of these are adenocarcinomas [3]. The discovery of the epidermal growth factor receptor gene (*EGFR*) mutation in patients with lung adenocarcinomas in 2004 [4-6] and the evolution of genomic sequencing and targeted therapy have resulted in the further subclassification of lung adenocarcinomas based on the presence of driver oncogenes.

The human epidermal growth factor receptor 2 gene (*HER2/ERBB2*) is an important driver oncogene for lung adenocarcinomas. *HER2*, the protein encoded by this gene, is a tyrosine kinase receptor of the *ErbB* family. *HER2* has no direct activating ligand; it serves as the preferred and most stable hetero-dimerization partner for all the other family receptors, especially *EGFR*. *HER2* dysregulation presents itself as HER2 protein overexpression in 6% to 35% of non-small cell lung cancer, gene amplification in 10% to 20%, and *HER2* mutations in 2% to 4% [7, 8], resulting in constitutive activation of intracellular signaling through the PI3K/AKT/mTOR and MEK/ERK pathways, and subsequently promoting cellular mitosis and proliferation [9, 10].

As new drug development for *HER2*-mutant lung cancers is accelerating, it is increasingly important to study the unique characteristics of this group of patients [7, 11, 12]. Radiogenomics is the study of the radiological appearance of tumors in association with genomic alterations, including driver oncogenes [13]. It is highly promising for the follow-up assessment of tailored targeted therapies. Rizzo et al. has noted a preponderance for air bronchograms, pleural retractions, small lesion size, and absence of fibrosis for *EGFR*-mutant lung adenocarcinomas; and a round lesion shape for *KRAS*-mutant adenocarcinomas in addition to presence of nodules in non-tumor lobes [14]. As such the goal of this study was to identify the radiologic characteristics of *HER2*-mutant lung adenocarcinomas in comparison with other non-small cell lung cancer subtypes, specifically *KRAS*- and *EGFR*-mutant lung adenocarcinomas.

2. Materials and methods

2.1. Patient selection

We undertook this retrospective study at our institution, a tertiary cancer referral center. The study was approved by our Institutional Review Board and was compliant with the

Health Insurance Portability and Accountability Act. Patient informed consent was waived and all data collected for this study were de-identified. We screened our institutional database for consecutive patients with biopsy-proven lung adenocarcinomas of any stage with *HER2* mutations seen in the thoracic oncology service between February 9, 2007, and August 17, 2015. All patients had also undergone molecular profiling performed by the Department of Pathology using a number of assays: fragment analysis, Sanger sequencing, Sequenom hotspot testing or broad, hybrid-capture next-generation sequencing (MSK-IMPACT, Illumina HiSeq). Of all potentially eligible *HER2* patients, only patients with at least one available pre-biopsy CT scan on our institutional Picture Archiving and Communication System (PACS, GE Centricity RA1000, GE Healthcare, Chicago, IL) were included in the study. Therefore, the final *HER2* population for this study consisted of 50 patients. In addition, we searched our database for NSCLC patients with *KRAS* or *EGFR* mutations to serve as control groups, since *HER2* mutations are generally considered mutually exclusive with these mutations in lung adenocarcinomas. These controls were stage-matched with the *HER2* mutation cohort. The final study population consisted of 154 patients. We recorded patient clinical information retrieved from our electronic medical record, such as age, sex, and stage of disease. There was no prior or current treatment for lung cancer in our selected patients.

2.2. Image analysis

The earliest available CT scan before biopsy was selected. Two junior radiologists (P.S. and A.L.) reviewed each CT separately, and then two senior thoracic radiologists (A.P. and M.G.) with post-fellowship experience (4 and 21 years of experience respectively) reviewed each CT scan to establish a consensus read. All readers were blinded to clinical data and molecular features at the time of image analysis. All images were reviewed on our institutional PACS. CT slice thickness varied from 0.625 mm to 2.5 mm in twenty-five patients (16%) and from 3 mm to 5 mm in one hundred and twenty-nine patients (84%). Seventy-four patients (48%) received intravenous contrast. The CT scans were performed on either a 16- or 64-slice CT scanner.

2.2.1. Radiologic features of the primary lung tumor—The size of the primary tumor was measured on lung windows by drawing the longest axis for length and then taking the longest perpendicular distance to determine the width [15]. The primary tumor was classified as central, peripheral or indeterminate. A lesion contacting a central bronchus to the lobar level was identified as central; lesions distal to this level were defined as peripheral; and if the lesion spanned both central and distal locations, it was labeled indeterminate [16]. The consistency of the primary tumor was also characterized as "solid" (density obscuring underlying pulmonary vessels and parenchyma), "ground glass" (increased attenuation of the lung parenchyma without obscuring the underlying pulmonary vessels and parenchyma), "mixed," or "consolidation." The contour of the primary tumor was described as either "round/oval" with well-defined smooth margins, "lobulated" with well-defined smooth margins, "speculated", or as a "mass-like consolidation." Finally, additional findings were recorded such as the presence of cavitation, air bronchograms, calcifications (intra-lesional densities   100 Hounsfield units), necrosis, postobstructive

atelectasis, chest wall invasion, lymphangitic spread, pleural tags (linear centrifugal extensions to the pleura or fissure), and pleural retractions.

2.2.2.   Ancillary characteristics—Additional ancillary findings were recorded such as the presence of ipsilateral hilar (N1 stage), mediastinal or scalene/supraclavicular lymphadenopathy (N3 stage) (measuring   1 cm in short axis, rounded, necrotic, enhancing and with loss of fatty hilum [17]); pleural effusion size and laterality; and lung metastases (satellite versus distant nodules).

2.3.   Statistical analysis

HER2 patients were stage-matched (stages IA, IB, IIA, IIB, versus stages IIIA and IIIB, versus stage IV) with controls carrying KRAS mutations as well as separately with controls carrying EGFR mutations using the greedy method [18]. In the case of ties, the first encountered control was chosen by the algorithm.

The Wilcoxon rank-sum test was used to compare continuous characteristics (age, size) between groups, while Fisher's exact test was used to assess the associations between categorical features and the different mutant groups, p values of < 0.05 were considered significant.

3.   Results

3.1.   Patient characteristics

One hundred and fifty-four patients with lung adenocarcinoma were identified: 50 (33%) patients with *HER2* mutations, 56 (36%) patients with *KRAS* mutations, and 48 (31%) patients with sensitizing *EGFR* mutations. Patients with *HER2*-mutant lung cancers were predominantly female (n = 36, 72%), with a median age of 61.6 years (range, 37.7–84.4), 50% (n = 25) of whom presented with stage 4 disease. Patients with *KRAS*-mutant lung cancers were predominantly female (n = 30, 54%), with a median age of 69.6 years (range, 38.6–86.3) and stage 4 disease at time of presentation (n = 27, 48%). Patients with *EGFR*-mutant lung cancers were predominantly female (n = 34, 71%), with a median age of 67.7 years (range, 37.7–87.0) and stage 4 disease at time of presentation (n = 20, 42%).

Comparisons between the *HER2*-mutant adenocarcinoma group and control groups showed a statistically significant difference in age (61.6 versus 69.6 years, $p = 0.009$ compared with the *KRAS*-mutant group; and 61.6 versus 67.7 years, $p = 0.03$ compared with the *EGFR*-mutant group), and approaching significance in predilection for the female sex (72% versus 54%, $p = 0.07$ compared with the *KRAS*-mutant group). Detailed findings are listed in Table 1.

3.2.   CT scan findings

3.2.1.   Radiologic features of HER2-mutant lung cancers—Lung cancers with *HER2* mutations were frequently peripheral (n = 35, 70%), solid in consistency (n = 33, 66%), spiculated in contour (n = 27, 54%), and were notable for the presence of pleural tags (n = 37, 74%) and pleural retractions (n = 29, 58%) (Figs. 1 and 2). Less commonly, they

showed air bronchograms (n = 17, 34%), demonstrated cavitation (n = 3, 6%), calcification (n = 2, 4%), < 50% necrosis (n = 3, 6%) and post obstructive atelectasis (n = 5, 10%). Common ancillary findings were lymphadenopathy (mediastinal n = 24, 48%; ipsilateral hilar n = 18, 36%; and N3 adenopathy n = 12, 24%), ipsilateral pleural effusion (n = 10, 20%; Fig. 3) as well as satellite and distant lung nodules (n = 12, 24% and n = 14, 28%, respectively). Findings are summarized in Table 2.

3.2.2.   Comparison with control groups—There was a significant difference between *HER2*-mutant adenocarcinoma group and the *KRAS*-mutant control group in terms of the axial length and width of the tumor (2.3 cm versus 2.9 cm, $p = 0.005$ for length; 1.6 cm versus 2.1 cm, $p = 0.002$ for width), the presence of pleural tags (74% versus 52%, $p = 0.03$), pleural retractions (58% versus 39%, $p = 0.006$), ipsilateral hilar adenopathy (36% versus 16%, $p = 0.03$), and N3 adenopathy (24% versus 7%, p = 0.03). In addition, there was a prevalence of pleural retractions in *HER2*-mutant tumors compared with the *EGER*-mutant control group (58% versus 37%, $p = 0.05$). On the other hand, no significant statistical difference between patients with *HER2* mutation and *KRAS* mutation regarding the peripheral location (70% versus 86%, $p = 0.06$) and solid consistency (66% versus 82%; $p = 0.06$) of the primary tumor with these characteristics being exhibited less often in *HER2*-mutant adenocarcinomas compared with the *KRAS* control group. Similarly, no significant difference was noted when other features were compared (Table 2).

4.   Discussion

HER2 gene dysregulation is a known driver of tumor growth and has been identified in several human malignancies, mainly breast, stomach and lung cancers [19-21]. In lung cancer, cancers harboring *HER2* mutations can be aggressive, portending a poor prognosis [9, 22]. Mazières et al. described three major types of *HER2* dysregulation in patients with non-small cell lung cancer that may increase oncogenic signaling independent from *EGFR* and *KRAS* mutations, and *ALK* fusions. The most common dysregulation is HER2 protein overexpression (6–35%), followed by *HER2* gene amplification (2–5%) and *HER2* gene mutation (2–4%) [7, 8]. At the same time, however, these cancers might benefit from existing and emergent therapies targeting HER2, especially when combined with conventional chemotherapy [11]. Novel *HER2*-targeted drugs are being tested and encouraging activity has been seen [16, 23]. A phase II trial in *HER2* exon 20 insertion-containing lung cancers showed single agent activity of dacomitinib, a pan-*HER* inhibitor that binds irreversibly to *HER2*, *HER1* (*EGFR*), and *HER4* tyrosine kinases receptors [12]. A more recent phase II trial of ado-trastuzumab emtansine was declared positive after demonstrating 44% partial response rate in patients with *HER2*-mutant lung cancers [24]. Lately, radiogenomics has taken radiology a step beyond its conventional descriptive role. The power to see the genomic characteristics of various tumors plays a pivotal role in engineering an adequate targeted therapy in various cancers including lung adenocarcinoma [25-29], and predicting their response to treatment [32]. To our knowledge, our study is the first to describe the CT characteristics of *HER2*-mutant lung adenocarcinomas. Several other studies have examined the radiologic characteristics of NSCLCs associated with other driver oncogenes. A similar study conducted by Yano et al. for *EGFR*-mutant NSCLC found

a predilection for solid nature [30] and others found a correlation between the size of the primary tumor, its ground glass component, and the probability of harboring *EGFR* mutation [31].

In our study, we found that *HER2*-mutant lung cancers occurred commonly in female patients with an advanced stage at time of diagnosis and in a relatively younger age group. Previously, Mazières et al. [8] obtained comparable epidemiological findings, including a median age of 60 years, a high proportion of women (69%), and a high proportion of stage 4 disease at presentation (50%) were found in *HER2*-mutant NSCLCs. In addition, they and others noted similar observations regarding the predilection of patients with *HER2*-mutant lung cancers to present in younger females with predominantly stage 4 disease at the time of diagnosis, in addition to a history of minimal to no tobacco exposure [8, 32, 33].

Radiologically, our study also showed that *HER2*-mutant tumors were significantly associated with a preference for peripheral location, solid consistency, and spiculated contour. When *HER2*-mutant tumors were compared with the *KRAS*-mutant control group, they were significantly smaller in size, associated with pleural retractions, more frequent air bronchograms, and a prevalence of pleural tags. In addition, more local (ipsilateral hilar, N1 level) and N3 adenopathy were found with *HER2*-mutant tumors versus the *KRAS*-mutant control group.

The preponderance of pleural tags and retractions in *HER2*-mutant adenocarcinoma might point toward its locally-invasive nature. Furthermore, the more frequent nodal involvement might also point toward the aggressive behavior and early nodal spread of these tumors. In fact, a plausible analogy can be drawn with inflammatory breast cancer which exhibits *HER2* amplification in approximately 40% of cases [34], and which tends to pursue an aggressive course with lymphangitic spread, pleural disease, and local invasion. A meta-analysis conducted by Elias et al. regarding the various radiologic characteristics of HER2-positive breast cancers shows the strong association between HER2 overexpression and indistinct masses with irregular margins on mammography, ultrasound, and magnetic resonance imaging [25].

The major limitations of our study are the relatively small sample size and its retrospective nature. Because of the low incidence of these genomic events, larger multicenter trials will be required to better describe and consolidate these radiological findings. Moreover, due to the relatively small sample size and the limited pool of controls, we did not adjust for multiple testing due to the exploratory nature of the study; therefore, results should be interpreted with caution, and validation is needed in future studies. In addition, the prevalence of an advanced stage at time of diagnosis (stage 4) for the *HER2*-mutant and control groups might represent a confounding factor due to lead time bias, since with advanced stage, different radiological features may overlap and co-exist irrespective of the oncogene. By stage-matching the patients, we tried to diminish such possible effects. On another note, the studied CT scans show a varying slice thickness from 0.625 mm to 5 mm, so that lack of thin slices in some scans might have limited evaluation of tumor features. Finally, the wide array of *HER2* mutation subtypes might represent an intrinsic heterogeneity factor in our studied group; an interesting area for future studies is to delve

into the most common and significant molecular dysregulations of the *HER2* oncogene such as exon 20 insertion YVMA [16].

In conclusion, lung adenocarcinomas harboring *HER2* mutation display several radiological features that may highlight the aggressive behavior of the primary tumor and its nodal metastatic spread. Moreover, it shares many of its epidemiological and radiographic characteristics with adenocarcinomas harboring other mutations (such as those involving *KRAS* and *EGFR*). The continuous advances in molecular and genomic sequencing, in addition to the growing field of radiogenomics, may play a pivotal role in the future characterization of these tumors radiologically.

Acknowledgments

References

[1]. World Health Organization. Cancer fact sheet February 2017 [cited 2017 6/1/2017]; Available from:, http://www.who.int/mediacentre/factsheets/fs297/en/; 2017.

[2]. American Cancer Society. Lung cancer (non-small cell) [1/5/2017 6/1/2017]; Available from:, https://www.cancer.org/cancer/non-small-cell-lung-cancer/about/key-statistics.html; 2017.

[3]. American Cancer Society. What is non-small cell lung cancer? [6/1/2017]; Available from:, https://www.cancer.org/cancer/non-small-cell-lung-cancer/about/what-is-non-small-cell-lung-cancer.html; 2016.

[4]. Lynch TJ, et al. Activating mutations in the epidermal growth factor receptor underlying responsiveness of non-small-cell lung cancer to gefitinib. N Engl J Med 2004;350(21):2129–39. [PubMed: 15118073]

[5]. Paez JG, et al. EGFR mutations in lung cancer: correlation with clinical response to gefitinib therapy. Science 2004;304(5676): 1497–500. [PubMed: 15118125]

[6]. Pao W, et al. EGF receptor gene mutations are common in lung cancers from "never smokers" and are associated with sensitivity of tumors to gefitinib and erlotinib. Proc Natl Acad Sci U S A 2004;101(36):13306–11. [PubMed: 15329413]

[7]. Li BT, et al. HER2 amplification and HER2 mutation are distinct molecular targets in lung cancers. J Thorac Oncol 2016;11(3):414–9. [PubMed: 26723242]

[8]. Mazieres J, et al. Lung cancer that harbors an HER2 mutation: epidemiologic characteristics and therapeutic perspectives. J Clin Oncol 2013;31 (16): 1997–2003. [PubMed: 23610105]

[9]. Takezawa K, et al. HER2 amplification: a potential mechanism of acquired resistance to EGFR inhibition in EGFR-mutant lung cancers that lack the second-site EGFRT790M mutation. Cancer Discov 2012;2(10):922–33. [PubMed: 22956644]

[10]. Pallis AG, Syrigos KN. Lung cancer in never smokers: disease characteristics and risk factors. Crit Rev Oncol Hematol 2013;88(3):494–503. [PubMed: 23921082]

[11]. Eng J, et al. Outcomes of chemotherapies and HER2 directed therapies in advanced HER2-mutant lung cancers. Lung Cancer 2016;99:53–6. [PubMed: 27565914]

[12]. Kris MG, et al. Targeting HER2 aberrations as actionable drivers in lung cancers: phase II trial of the pan-HER tyrosine kinase inhibitor dacomitinib in patients with HER2-mutant or amplified tumors. Ann Oncol 2015;26(7): 1421–7. [PubMed: 25899785]

[13]. Mazurowski MA. Radiogenomics: what it is and why it is important. J Am Coll Radiol 2015;12(8):862–6. [PubMed: 26250979]

[14]. Rizzo S, et al. CT radiogenomic characterization of EGFR, K-RAS, and ALK mutations in non-small cell lung cancer. Eur Radiol 2016;26(1):32–42. [PubMed: 25956936]

[15]. McErlean A, et al. Intra- and interobserver variability in CT measurements in oncology. Radiology 2013;269(2):451–9. [PubMed: 23824993]

[16]. Plodkowski AJ, et al. From genotype to phenotype: are there imaging characteristics associated with lung adenocarcinomas harboring RET and ROS1 rearrangements? Lung Cancer 2015;90(2):321–5. [PubMed: 26424208]

[17]. Kramer H, Groen HJ. Current concepts in the mediastinal lymph node staging of nonsmall cell lung cancer. Ann Surg 2003;238(2): 180–8. [PubMed: 12894010]

[18]. Bergstralh EJ, Kosanke JL, Jacobsen SJ. Software for optimal matching in observational studies. Epidemiology 1996;7(3):331–2. [PubMed: 8728456]

[19]. Gravalos C, Jimeno A. HER2 in gastric cancer: a new prognostic factor and a novel therapeutic target. Ann Oncol 2008;19(9):1523–9. [PubMed: 18441328]

[20]. Slomovitz BM, et al. Her-2/neu overexpression and amplification in uterine papillary serous carcinoma. J Clin Oncol 2004;22(15):3126–32. [PubMed: 15284264]

[21]. Scholl S, Beuzeboc P, Pouillart P. Targeting HER2 in other tumor types. Ann Oncol 2001;12(Suppl l):S81–7. [PubMed: 11521727]

[22]. Takeuchi K, et al. RET, ROS1 and ALK fusions in lung cancer. Nat Med 2012; 18(3): 378–81. [PubMed: 22327623]

[23]. Mazieres J, et al. Lung cancer patients with HER2 mutations treated with chemotherapy and HER2-targeted drugs: results from the European EUHER2 cohort. Ann Oncol 2016;27(2):281–6. [PubMed: 26598547]

[24]. Li BT, et al. Ado-trastuzumab emtansine in patients with HER2 mutant lung cancers: results from a phase II basket trial. J Clin Oncol 2017;35(15_suppl):8510.

[25]. Elias SG, et al. Imaging features of HER2 overexpression in breast cancer: a systematic review and meta-analysis. Cancer Epidemiol Biomarkers Prev 2014;23(8): 1464–83. [PubMed: 24807204]

[26]. Wang R, et al. RET fusions define a unique molecular and clinicopathologic subtype of non-small-cell lung cancer. J Clin Oncol 2012;30(35):4352–9. [PubMed: 23150706]

[27]. Choi C-M, et al. Advanced adenocarcinoma of the lung: comparison of CT characteristics of patients with anaplastic lymphoma kinase gene rearrangement and those with epidermal growth factor receptor mutation. Radiology 2015;275(1): 272–9. [PubMed: 25575117]

[28]. Halpenny DF, et al. Are there imaging characteristics associated with lung adenocarcinomas harboring ALK rearrangements? Lung Cancer 2014;86(2):190–4. [PubMed: 25312988]

[29]. Halpenny DF, et al. Radiogenomic evaluation of lung cancer — are there imaging characteristics associated with lung adenocarcinomas harboring BRAF mutations? Clin Imaging 2017;42:147–51. [PubMed: 28012356]

[30]. Glynn C, Zakowski MF, Ginsberg MS. Are there imaging characteristics associated with epidermal growth factor receptor and KRAS mutations in patients with adenocarcinoma of the lung with bronchioloalveolar features? J Thorac Oncol 2010;5(3):344–8. [PubMed: 20087229]

[31]. Yano M, et al. Epidermal growth factor receptor gene mutation and computed tomographic findings in peripheral pulmonary adenocarcinoma. J Thorac Oncol 2006; 1(5): 413–6. [PubMed: 17409892]

[32]. Mar N, Vredenburgh JJ, Wasser JS. Targeting HER2 in the treatment of non-small cell lung cancer. Lung Cancer 2015;87(3):220–5. [PubMed: 25601485]

[33]. Pao W, Girard N. New driver mutations in non-small-cell lung cancer. Lancet Oncol 2011;12(2): 175–80. [PubMed: 21277552]

[34]. Bertucci F, et al. Gene expression profiling identifies molecular subtypes of inflammatory breast cancer. Cancer Res 2005;65(6):2170–8. [PubMed: 15781628]

Fig. 1.
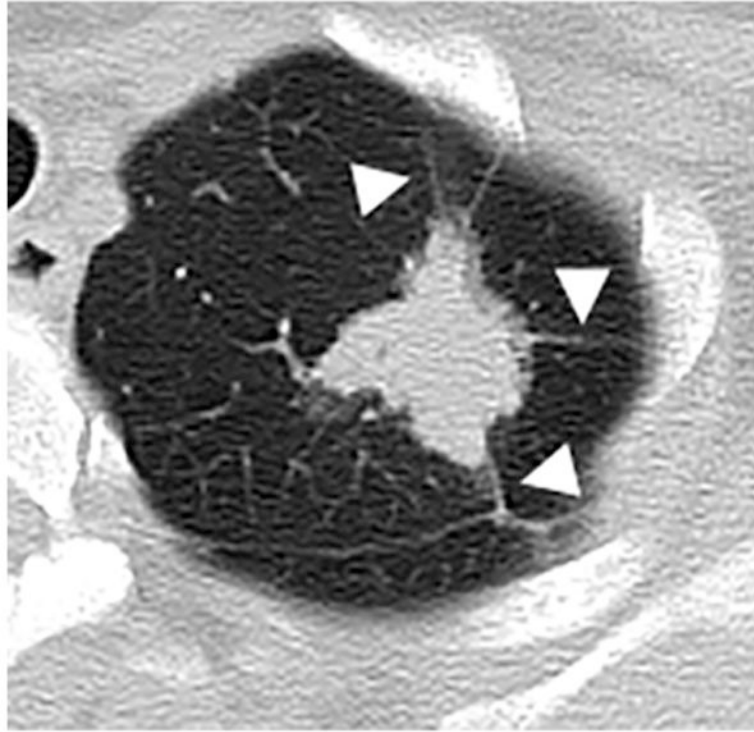Pleural tags (white arrowheads) in a patient with *HER2*-mutant lung adenocarcinoma.

Fig. 2.
Pleural retraction (black arrowhead) and air bronchograms (black arrows) in a patient with *HER2*-mutant lung adenocarcinoma.

Fig. 3.
Subcarinal mediastinal (N2 level) and ipsilateral hilar (N1 level) adenopathy (white arrows) and a pleural effusion (black arrow) in a patient with *HER2*-mutant lung adenocarcinoma.

Table 1

Characteristics of patients with *HER2-, KRAS-,* and *EGFR*-mutant lung cancers.

	Mean (range) or n (%)				*p* value	
	All (n = 154)	KRAS (n = 56)	EGFR (n = 48)	HER2 (n = 50)	KRAS vs HER2	EGFR vs HER2
Age, years	66.4 (37.4, 87.0)	69.6 (38.6, 86.3)	67.7 (37.4, 87.0)	61.6 (37.7, 84.4)	0.009 [*]	0.03 [*]
Gender					0.07	1.00
Female	100 (65%)	30 (54%)	34 (71%)	36 (72%)		
Male	54 (35%)	26 (46%)	14 (29%)	14 (28%)		
Stage					0.97	0.82
1A	37 (24%)	13 (23%)	13 (27%)	11 (22%)		
IB	9 (6%)	4 (7%)	3 (6%)	2 (4%)		
2A	1 (1%)	0 (0%)	1 (2%)	0 (0%)		
2B	1 (1%)	0 (0%)	0 (0%)	1 (2%)		
3A	21 (13%)	7 (13%)	8 (17%)	6 (12%)		
3B	13 (8%)	5 (9%)	3 (6%)	5 (10%)		
4	72 (47%)	27 (48%)	20 (42%)	25 (50%)		

[*] Significant at $p < 0.05$.

Table 2

Radiologic features of *HER2-, KRAS-,* and *EGFR*-mutant lung cancers by computed tomography.

	Median (range in cm)			Wilcoxon rank-sum test *p*-value	
	HER2 (n = 50)	**KRAS (n = 56)**	**EGFR (n = 48)**	**KRAS vs HER2**	**EGFR vs HER2**
Mass axial length	2.3 (0.4, 8.5)	2.9 (0.8, 6.9)	3.3 (0.8, 9.2)	0.005 *	0.13
Mass axial width	1.6 (0.4, 7.8)	2.1 (0.8, 5.7)	2.3 (0.6, 7.8)	0.002 *	0.23
	n (%)			Fisher's exact test *p* value	
	HER2 (n = 50)	**KRAS (n = 56)**	**EGFR (n = 48)**	**HER2 vs KRAS**	**HER2 vs EGFR**
Central location					
No	39 (78)	51 (91)	42 (88)	0.10	0.29
Yes	11 (22)	5 (9)	6 (12)		
Peripheral location					
No	15 (30)	8 (14)	10 (21)	0.06	0.36
Yes	35 (70)	48 (86)	38 (79)		
Indeterminate location					
No	47 (94)	53 (95)	44 (92)	1.00	0.71
Yes	3 (6)	3 (5)	4 (8)		
Consistency					
Solid	33 (66)	46 (82)	32 (67)	0.06	0.72
Mixed solid/ground-glass	9 (18)	8 (14)	11 (23)		
Consolidation	8 (16)	3 (4)	5 (10)		
Contour					
Round/oval	5 (10)	8 (14)	10 (21)	0.22	0.42
Lobulated	9 (18)	10 (18)	9 (19)		
Spiculated	27 (54)	35 (63)	24 (50)		
Mass-like consolidation	9 (18)	3 (5)	5 (10)		
Cavitation					
No	47 (94)	55 (98)	46 (96)	0.34	1.00
Yes	3 (6)	1 (2)	2 (4)		
Air bronchograms					
No	33 (66)	51 (91)	37 (77)	0.002 *	0.27
Yes	17 (34)	5 (9)	11 (23)		
Calcification					
No	48 (96)	53 (95)	45 (94)	1.00	0.67
Yes	2 (4)	3 (5)	3 (6)		
Post obstructive atelectasis					
No	45 (90)	53 (95)	44 (92)	0.47	1.00
Yes	5 (10)	3 (5)	2 (8)		
Pleural tags					

	Median (range in cm)			Wilcoxon rank-sum test p-value	
	HER2 (n = 50)	*KRAS* (n = 56)	*EGFR* (n = 48)	*KRAS* vs *HER2*	*EGFR* vs *HER2*
No	13 (26)	27 (48)	20 (42)	0.03 *	0.13
Yes	37 (74)	29 (52)	28 (58)		
Pleural retraction					
No	21 (42)	39 (70)	30 (63)	0.006 *	0.05
Yes	29 (58)	17 (39)	18 (37)		
Lymphangitic spread					
No	40 (80)	51 (91)	44 (92)	0.16	0.15
Yes	10 (20)	5 (9)	4 (8)		
Satellite nodules					
No	38 (76)	40 (71)	35 (73)	0.66	0.82
Yes	12 (24)	16 (29)	13 (27)		
Nodules in a different lobe					
No	36 (72)	39 (70)	39 (81)	0.83	0.34
Yes	14 (28)	17 (30)	9 (19)		
Necrosis					
None	47 (94)	53 (95)	45 (94)	0.29	1.00
< 50%	3 (6)	1 (2)	3 (6)		
50–100%	0 (0)	2 (3)			
Chest wall invasion					
No	50 (100)	55 (98)	48 (100)	1.00	NA
Yes	0 (0)	1 (2)	0 (0)		
Mediastinal lymph nodes					
No	26 (52)	37 (66)	31 (65)	0.17	0.23
Yes	24 (48)	19 (34)	17 (35)		
Ipsilateral hilar N1 lymph nodes					
No	32 (64)	47 (84)	37 (77)	0.03 *	0.19
Yes	18 (36)	9 (16)	11 (23)		
Supraclavicular/scalene N3 lymph nodes					
No	38 (76)	52 (93)	42 (88)	0.03 *	0.19
Yes	12 (24)	4 (7)	6 (12)		
Effusion ipsilateral					
None	40 (80)	48 (86)	44 (92)	0.51	0.14
Small/moderate	9 (18)	8 (14)	3 (6)		
Large	1 (2)	0 (0)	1 (2)		
Effusion contralateral					
None	49 (98)	54 (96)	48 (100)	1.00	1.00
Small/moderate	1 (2)	2 (4)	0 (0)		

*
Significant at $p < 0.05$.